Abdominal Radiology

Published online: 20 June 2018

Abdom Radiol (2019) 44:2021–2029
https://doi.org/10.1007/s00261-018-1660-7

Radiomics and radiogenomics of prostate cancer

Clayton P. Smith,[1,2] Marcin Czarniecki,[1] Sherif Mehralivand,[1,3,4] Radka Stoyanova,[5] Peter L. Choyke,[1] Stephanie Harmon,[6] and Baris Turkbey[1]

[1]Molecular Imaging Program, National Cancer Institute, NIH, 10 Center drive, room B3B85, Bethesda, MD 20892, USA
[2]Georgetown University School of Medicine, Washington, DC, USA
[3]Urologic Oncology Branch, National Cancer Institute, NIH, Bethesda, MD, USA
[4]Department of Urology and Pediatric Urology, University Medical Center Mainz, Mainz, Germany
[5]Department of Radiation Oncology, University of Miami Miller School of Medicine, Miami, FL, USA
[6]Clinical Research Directorate/Clinical Monitoring Research Program, Leidos Biomedical Research, Inc, NCI Campus at Frederick, Frederick, MD, USA

Abstract

Radiomics and radiogenomics are attractive research topics in prostate cancer. Radiomics mainly focuses on extraction of quantitative information from medical imaging, whereas radiogenomics aims to correlate these imaging features to genomic data. The purpose of this review is to provide a brief overview summarizing recent progress in the application of radiomics-based approaches in prostate cancer and to discuss the potential role of radiogenomics in prostate cancer.

Key words: Prostate cancer—Imaging—Radiomics—Radiogenomics

The recent shift in interest from qualitative interpretation of medical imaging to an emphasis on extraction of quantitative information from medical imaging (*radiomics*) is driven by the hypothesis that macroscopic heterogeneity on imaging reflects biological diversity of underlying disease [1, 2]. The application of radiomics in localized prostate cancer is particularly attractive given the widespread, yet underutilized, use of imaging. Currently, the primary method of risk stratification in men diagnosed with localized prostate cancer is pathological grading from biopsy samples, serum PSA levels, and clinical staging [3]. However, challenging anatomy and limited tissue acquisition leads to a spatial sampling bias when using standard biopsy techniques. Numerous studies have demonstrated an underestimation of adverse pathology in up to 38–46% of patients when biopsies are randomly acquired and up to 23% when targeted based on imaging findings [4–6]. This high rate of misclassification is suspected to be caused by spatial heterogeneity of morphological growth patterns within cancerous lesions [7, 8]. In addition to morphological variation, a growing body of evidence supports the existence of substantial genetic heterogeneity across prostate cancer lesions within the same patient [9]. Taken together, undersampling biological heterogeneity could lead to underestimation of risk-assessment in localized disease, thus necessitating prognostic tests that can fully sample, or supplement, current biopsy-based methods of disease characterization.

Imaging is unique in that it can overcome the aforementioned sampling bias by providing a non-invasive platform for assessing the entire burden of a patient's disease, sampling both inter- and intra-lesion heterogeneity. Multiparametric magnetic resonance imaging (mpMRI) has become a standard imaging modality for detection of localized disease, demonstrating high sensitivity in detection and localization of prostate cancer lesions [10]. Despite this high sensitivity, mpMRI is limited by false positives due to benign pathologies and high inter-reader variability in interpretation and adherence to qualitative reporting paradigms [11]. The use of quantitative imaging characteristics is motivated by the correlation of signal intensity of multiple mpMRI pulse sequences, such as T2-weighted (T2W) imaging and diffusion-weighted imaging, with nuclear density of cells

Peter L. Choyke, Stephanie Harmon and Baris Turkbey share the senior authorship.

Correspondence to: Baris Turkbey; *email:* turkbeyi@mail.nih.gov

on pathological assessment [12–14]. However, signal intensity alone is yet to lead to accurate prediction and characterization of pathological grade.

Overall, there are several unmet needs in the detection and characterization of prostate cancer where radiomics-based approaches are uniquely suited to contribute to enhanced clinical prognostication and risk-assessment in patients with localized disease. To date, several groups have vested research interest in radiomics applications to prostate cancer imaging, including prostate segmentation, lesion detection, characterization, and classification (i.e., pathological grade prediction), as well as correlation to biological analyses such as genomics (*radiogenomics*). The purpose of this review is to provide a brief overview summarizing recent progress in the application of radiomics-based approaches in prostate cancer and to discuss the potential role of radiogenomics in prostate cancer.

What is radiomics?

Very simply, radiomics refers to the statistical derivation of extracting higher-order features from images [1]. There are several types of radiomics features that can be extracted from medical images based on the study task or research objective (Fig. 1). The selection and analysis of quantitative features remain a highly controversial topic in recent years due to the number of available features for use and variation in techniques for implementation [2]. Technical description and implementation of a radiomics analysis pipeline are out of the scope of this review; however, brief descriptions of radiomics features relevant to the studies evaluated are listed below. Methodologically, majority can be classified as either describing the intensity, texture, or shape of a region of interest:

- Intensity
  - Summary statistics of the intensity histogram within a given region, such as minimum, maximum, median, or mean
  - Metrics describing the skewness or kurtosis of intensity histogram within a region
- Texture
  - Gray-level co-occurrence matrix (GLCM) metrics: also known as Haralick features [15], these represent the most commonly used features, describing local texture based on the distribution of co-occurring value pairs within a given region
  - Fractal analysis: characterizes geometric complexity by describing spatial elements after images superimposed by various patterns [16]
  - Gabor transform: describes regional texture based on features derived from convolution of images with Gabor filters of varying scale and orientation [17]
  - Wavelet transform: describes regional texture derived from decomposition of original image based on filtering using complex linear or radial wavelets [18]
  - Other texture-based metrics derived from gray-level matrices include: Gray-level run-length matrix (GLRLM) [19], neighboring gray-level dependence matrix (NGLDM) [20], and neighborhood gray-tone difference matrix (NGTDM) [21]
- Shape
  - Summary statistics describing volume and/or size of a region, such as maximum axial length, maximum 3D diameter, surface area, and volume
  - Shape-based descriptors: sphericity, surface-to-volume ratio, spherical disproportion, and compactness

As radiomics features are statistically derived, as opposed to mechanistically defined, it is still unclear which features should be preferentially studied or how they relate back to a fundamental biological property. Before radiomics-based studies can truly be validated, uncertainties and robustness in the methodologies governing the extraction of higher-order features must be addressed. Researchers in the radiomics field should reference previous works highlighting the type-1 error inflation and cofounding statistical nature of high-dimensional feature space that contain inter-correlated elements [22, 23].

Potential uses of radiomics in prostate cancer

Prostate segmentation

Accurate prostate segmentation is important for many applications including radiation therapy planning, prebiopsy preparation, volume and PSA density estimation, and tumor localization [24–27]. Ultrasound is the most commonly used modality to image prostate gland due to its real-time realization and low cost [28]. Because of this, many researchers have attempted to create semi-automatic and automatic segmentation algorithms to decrease workload and standardize results [29–35]. These studies have shown variable results, limited by the quality of the ultrasound image and differing methodologies among studies. In the last decade, as MRI has become more widely adopted in the workup of prostate cancer (e.g., staging, treatment planning, treatment response) [36], segmentation research using MRI has recently intensified [37–39]. Like was done with ultrasound segmentation, many studies have tested both semi-automatic and automatic segmentation algorithms [40–44]. To streamline the radiotherapy planning process, Chowdhury et al. [38] built a linked statistical shape model (LSSM),

which links the shape variation of a structure of interest across multiple imaging modalities (MR and CT in this case). They compared multiple LSSMs to a CT statistical shape model (CTSSM, where only CT is utilized) and found that all the LSSMs performed both equally and superior to the CTSSM, suggesting the importance of using multiple imaging modalities to build a segmentation algorithm. Shiradkar et al. [39] created a multi-modal framework for detection of prostate cancer, segmentation of the gland, and generation of a radiomics-based dose plan on MRI for brachytherapy and on CT for external beam radiotherapy (EBRT) using the target delineations transferred from MRI to CT. The framework produces three dose plans: whole gland homogenous (the current clinical standard), radiomics-based focal, and whole gland with a radiomics-based focal boost. Comparisons of the three dose plans revealed that the radiomics targeted plans reduced dosage to organs at risk and boosted dose delivered to cancerous lesions.

Due to the difficulty in the testing of segmentation tools on multi-center, multi-vendor, and multi-protocol data, Litjens et al. [45] ran the PROMISE12 challenge for the comparison of MRI based segmentation methods. A total of 11 teams from different academic and industry groups participated, each having to use their algorithm on the same 100 prostate MR cases from 4 different centers. Algorithms varied in methods and implementation, including active appearance models, atlas registration, and level sets. Using boundary and volume based metrics to evaluate the algorithms, the challenge revealed that the two segmentation tools by Imorphics and ScrAutoProstate were significantly better than all other algorithms ($p < 0.05$) and had run times of 8 min and 3 s per case, respectively. Active appearance model based algorithms were overall superior in performance to other approaches like multi-atlas registration, both for accuracy and computation time. The authors concluded, however, that optimal performance is not yet obtained and that algorithm combination may lead to further improvement.

The prostate has two distinct regions observable on imaging: the peripheral zone (PZ), characterized by high signal on T2W MRI and the transition zone (TZ), which appears darker than the PZ on T2W MRI. T2W contrast in the prostate reflects the different amounts of macromolecular and free water present as the PZ is composed of highly glandular-ductal tissues appearing hyperintense on T2W MRI, while the TZ, composed of more stromal than ductal tissues, appears hypointense. The different imaging properties of the prostate zones are well recognized. More recently, several studies have provided segmentation of the prostate zonal structures [46–50].

Prostate cancer detection and classification

As with prostate segmentation tools, there have been many recent prostate cancer detection algorithms developed, also known as computer-aided diagnosis (CAD) systems [51–62]. CAD systems attempt to predict if and where cancer is present based on its analysis of at least one feature on MRI. It then usually develops a supervised classifier based on 'ground truth' cases, being trained on subsets of the data and then applied to the rest [63].

One of the earliest prostate CAD systems was developed by Madabhushi et al. [59]. They presented a method using 4 Tesla MRI *ex vivo* prostatectomy samples. In addition to first and second-order statistical methods, the authors used Gabor filters, discrete cosine transform, and Gradient based features to accomplish 98% specificity and 36–42% sensitivity.

Kwak et al. [56] used support vector machine (SVM) with local binary pattern features applied to T2W and b2000 images to predict the likelihood of cancer of each pixel. The authors trained the SVM on a cohort of 264 patients with recorded biopsy results. A recently developed prostate CAD by Lay et al. [57] extracted spatial, intensity, and texture features from T2W, ADC, and b2000 images using random forest classification to detect prostate cancer. The random forest considered instance-level weighting for equal treatment of small and large lesions and prostate backgrounds. This prostate CAD had a cancer detection AUC of 0.93, which performed better than the authors' previous SVM prostate CAD tested on the same data (AUC 0.86).

Radiomic features in singular sequences, or used in conjunction with mpMRI or with additional novel image acquisitions have been investigated if they may improve detection [55, 64, 65]. Khalvati et al. used mpMRI with additional calculated high-b value as well as correlated diffusion imaging (CDI), and compared the performance to classical sequences included in mpMRI [55]. The added parameters added to mpMRI were found to increase sensitivity, specificity, and AUC to 86, 82, and 86%, respectively which was better than mpMRI alone. The study though was not used by clinical reads by radiologists. Another study investigated a possible shorter scan time using only T2W and DWI, with the addition of texture analysis [66]. The study had the advantage of using clinical reads according to the PI-RADS criteria, and showed an improvement compared to PI-RADS with an AUC 0.87 vs. 0.73 for TZ and 0.89 vs. 0.76 for PZ, respectively. Similarly, Wang et al. demonstrated a higher sensitivity and specificity of a combined PI-RADS and radiomic analysis than any method alone (92.3% and 95.3%, respectively). None of these studies were externally validated to date, and were all performed on small sample sizes (< 100 cases) [65].

Additionally, textural features have shown associations between Gleason score assessment [67, 68]. Nketiah et al. have demonstrated that T2W textural features including angular second movement (a measure of homogeneity) and entropy (measuring randomness or

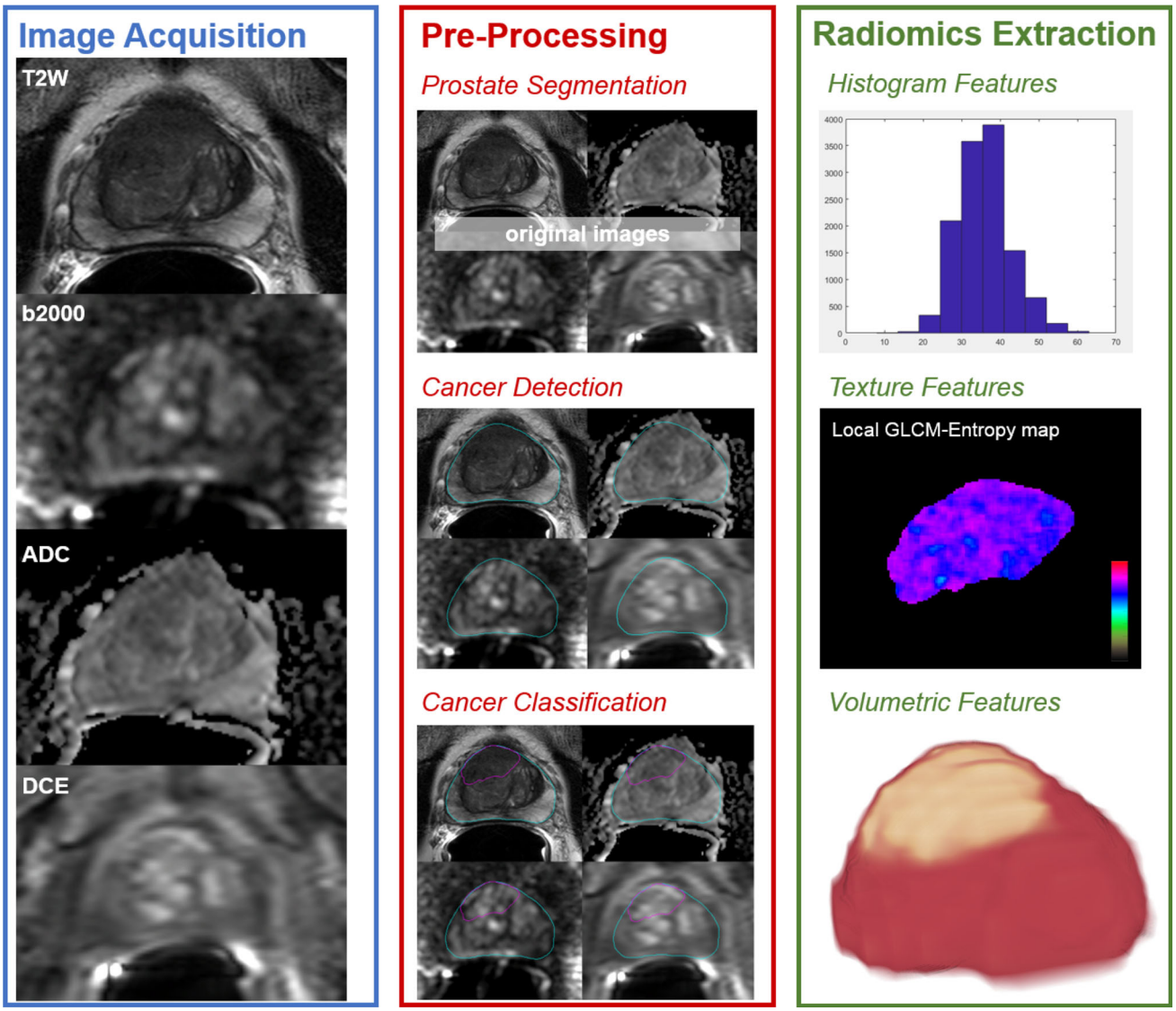

Fig. 1. Radiomics Workflow. Standard mpMRI protocol for prostate image includes T2-weighted (T2W) imaging, diffusion-weighted imaging (high *b* value [b2000], apparent diffusion coefficient [ADC]), and dynamic contrast-enhanced (DCE) imaging sequences. Pre-processing for radiomics-based analysis is task-specific. In applications of prostate volume segmentation, all (or parts) of the original imaging sequences are used for analysis. In applications for cancer detection and cancer classification, either the prostate volume (shown in blue) or the lesion volume (shown in pink) is used for refining areas of interest for radiomics-based analysis. Radiomics feature extraction can be completed on a voxel-basis or volumetric-basis depending on the technique. Shown is an example of feature extraction from the lesion ROI (pink), demonstrating the histogram of T2W signal, a voxel-based texture extraction (note for the purposes of this figure, 8-bit discretization and 7 × 7 neighborhood were used to derive GLCM matrix), and volumetric appearance.

complexity) were able to differentiate between Gleason 3 + 4 and Gleason 4 + 3 disease [68]. Fehr et al., could additionally show differences between Gleason 3 + 3 and higher Gleason scores (3 + 4 and 4 + 3 disease) using textural features from T2W and ADC alone [67]. Irrespective of the approach, the application of radiomics currently remains to be investigational techniques that require further validation and larger data trials.

Prostate MRI offers relatively high resolution to help in detection and localization of many smaller volume prostate cancer lesions, showing high sensitivity but low specificity and inter-reader agreement [69]. Prostate CAD systems show promise in the detection and diagnosis of cancer. Still, the field of prostate radiomics detection lacks standardized methodology and assessment of these investigations due to its rapid growth. This should be an area of focus for the field for its advancement as a discipline.

Radiogenomics in prostate cancer diagnostics

With more articles about radiomics in prostate cancer diagnostics being published in the recent years, another similar term, "radiogenomics", is becoming more visible in the literature [70–76]. Although easily confused with one another and often used interchangeably, both terms describe different fields in imaging diagnostics. Radiogenomics was initially described as a method of linking pre-treatment diagnostic imaging with genomic profiles associated with different toxic responses to radiation therapy. This has changed more recently, as current publications use more generalized definitions [72, 75]. The term radiogenomics is a morpheme combination of radiomics and genomics. Radiomics is a technical method of high-throughput extraction of imaging features from diagnostic images [74, 77–79]. These features can subsequently be used as non-invasive biomarkers in the detection [51, 55, 59, 80] as well as assessment of aggressiveness of prostate cancer [58, 64, 67, 81–83].

With increased use of mpMRI in detection and staging of prostate cancer, a larger amount of anatomic and functional imaging data have become available [6, 84–88]. Since mpMRI information is often used to obtain targeted biopsies of lesions and for staging of patients prior to surgery, larger amounts of imaging and histopathology data have become available. The genomics approach is another step towards personalized medicine which correlates genomic profiles, usually obtained from biopsy or surgery samples, with clinical outcomes. With the advent of high-throughput techniques like Microarrays [89, 90] and Next Generation Sequencing (NGS) [91–95], genomic analysis becomes broadly available. Radiogenomic methods utilize radiomics features to determine imaging biomarkers for the prediction of genomic profiles [70–73, 76, 77]. This method could potentially spare invasive diagnostic procedures in the sense of a non-invasive biopsy. Current data, however, are very limited with most studies being undertaken in lung cancer, glioblastoma multiforme, hepatocellular carcinoma, renal cancer, and gynecological cancers [71].

One of the first radiogenomics studies in prostate cancer was published by McCann et al. [96] in 2016. Thirty patients who underwent preoperative mpMRI and subsequent radical prostatectomy were retrospectively evaluated. Regions of interests (ROI) corresponding to tumor foci were manually contoured on 2D MRI images by a radiologist and pathologist. This was done in all anatomic and functional sequences of the MRI scan (T2W, diffusion-weighted, apparent diffusion coefficient, and dynamic contrast-enhanced MRI) and 45 cancer foci in the peripheral zone were finally identified. Six quantitative imaging features (mean ADC, ADC 10th percentile, skewness of T2W signal intensity, K_{trans}, V_e, and K_{ep}) were determined for every ROI and the corresponding pathology slides were identified by the pathologist. New slides were cut from the histopathology block and the specimens were stained by immunohistochemistry to determine Phosphatase and Tensin homolog (PTEN) expression. PTEN is a tumor suppressor gene on chromosome 10 and mutations or deletions have been associated with certain human cancers. The statistical methodology in this study was solely correlative and the main outcome was the correlation of quantitative imaging features with PTEN expression. It was stated that out of the six tested features only K_{ep} displayed a weak negative correlation with PTEN expression ($r = -0.35$, $p = 0.02$). All other features did not demonstrate a significant correlation. The authors explain this finding by the fact that PTEN is presumed to be a modulator of angiogenesis. Main limitations of this study include its retrospective design, small study population, no adjustment for multiple testing, no transition zone lesions, and no external validation.

Another radiogenomic study was published by Stoyanova et al. in 2016 [97]. Seventeen mpMRI-guided targeted biopsies from six patients were analyzed. The ROIs were identified retrospectively by reevaluating the needle paths of the MRI fusion-guided biopsies. Forty-nine different quantitative features extracted from 3D ROIs based on tumor volumes, intensity, perfusion, and diffusion were correlated with genomic profiles associated with poor outcome. The authors also included radiomics features from the Normal Appearing Tissue (NAT) in PZ and TZ. Three different commercially available genomic testing kits were tested (Decipher®, Polaris Cell Cycle Score [CCP®], and Genomic Prostate Score [GPS®]). These include genes that are either over- or under-expressed in aggressive prostate cancers. There were 445 significant correlations without adjusted p-values but even after adjustment for multiple testing, 64 correlations remained significant ($p < 0.05$) (Fig. 2). Furthermore, the authors performed gene ontology analysis showing correlation of radiomic features of the ROI and NAT with biological processes like immune response, metabolism, and cell and biological adhesion. Like the prior study main limitations were small population, retrospective design, and lack of external validation.

Although the notion of a non-invasive prediction of biopsy genomic data might sound tempting, it should be acknowledged that current data are very scarce. Most studies are retrospective and have low patient populations. Furthermore, radiogenomic studies are prone to statistical issues related to overfitted data and multiple testing [2, 98]. Thus, at present it is impossible to predict what role radiogenomics will ultimately play in prostate cancer diagnostics. Although current preliminary data are promising for some radiomic features it is also possible that prospective studies with larger patient populations will fail to prove a benefit. Future efforts should

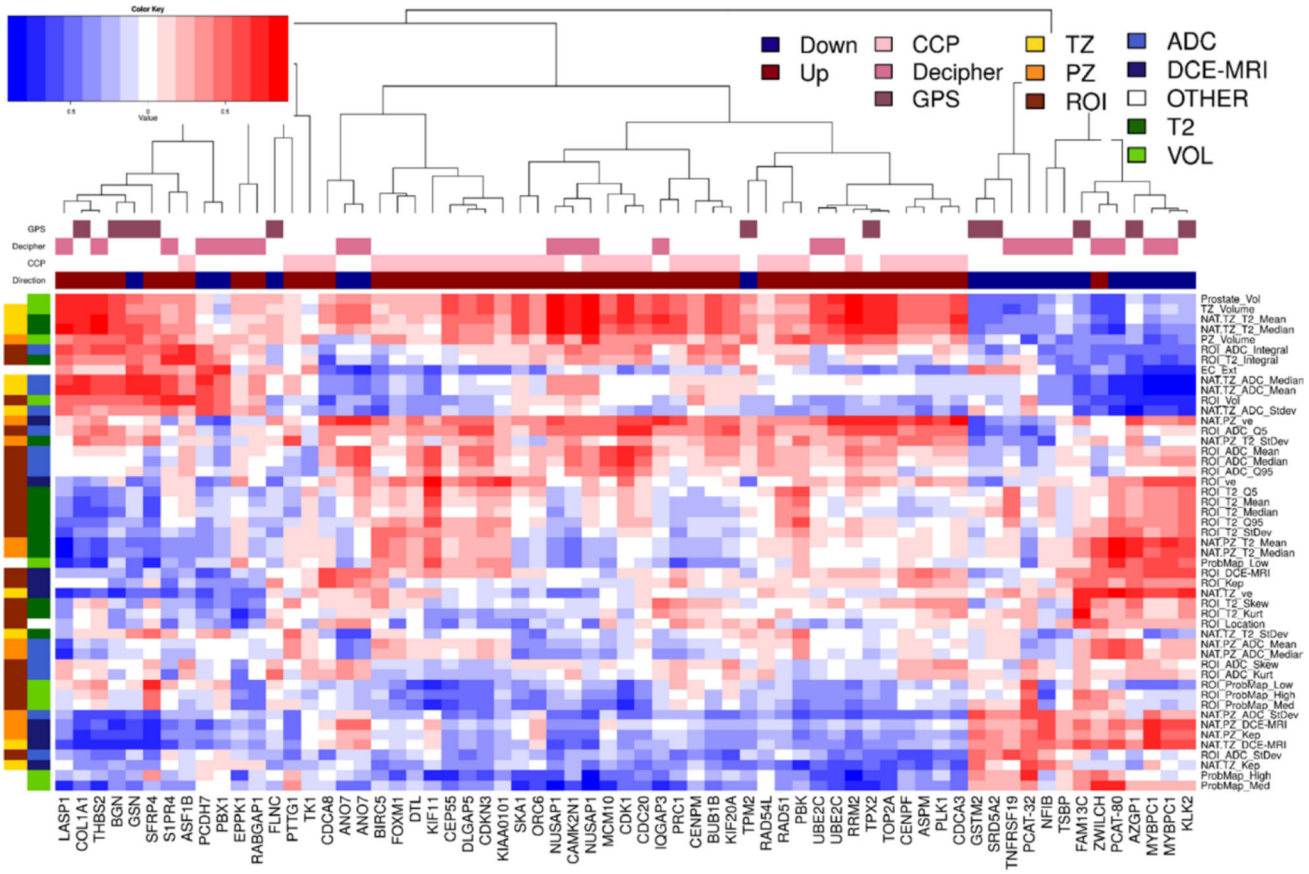

Fig. 2. Pearson's correlation analysis of imaging features and 65 genes from commercially available prostate cancer classifiers. Hierarchical clustering on Pearson's correlation distance between radiomic features and genes from commercially available prostate cancer classifiers: CCP (Cell Cycle Progression), Decipher, and GPS (Genomic Prostate Score). Genes in these signatures that are up-expressed in aggressive cancers are indicated by a dark red box over the gene's column while those that are down-expressed are indicated with a blue box. Groups of radiomic features are indicated along the dendrogram on the left. Group1 (left) connects the radiomic feature with location (TZ, PZ and ROI); Group 2 is related to the image modality/function: T2W, ADC and DCE-MRI. Reprinted from Stoyanova R et al. PMID: 27438142 with permission of Oncotarget.

therefore focus on acquisition of larger data quantity and initiation of prospective multi-center studies. With the availability of large imaging and genomic datasets in publicly available databases this could become more feasible in the near future [99, 100]. Furthermore, in the era of Big Data and Deep Machine Learning such data could be used to create computer-based decision support tools. Another important limitation is the lack of standardization. Imaging and reporting protocols differ significantly among institutions. The process of preparing imaging data (e.g., contouring of ROIs) is mainly done manually, which is cumbersome and prone to inter-user variability. Automatic and semi-automatic segmentation tools have been proposed and could not only simplify the process but also improve generalizability of results [98].

In summary, radiogenomics is a new and exciting approach that can take radiology to the next level from detection of cancer to prediction of genomic patterns which are related to different clinical outcomes. Current data in prostate cancer diagnostics are promising but limited and larger prospective studies with external validation are needed.

Conclusion

Radiomics and radiogenomics further evaluates the imaging phenotypes with correlation of biological and genomic features of prostate cancer with an ultimate goal of prediction of prognosis and treatment response. This relatively new branch of imaging sciences is evolving and is expected to play an important role in clinical management of prostate cancer. Further large scaled reproducible research is needed to accomplish this important goal.

Acknowledgements This project has been funded in whole or in part with federal funds from the National Cancer Institute, National Institutes of Health, under Contract No. HHSN261200800001E. The content of this publication does not necessarily reflect the views or policies of the Department of Health and Human Services, nor does mention of trade names, commercial products, or organizations imply endorsement by the U.S. Government. This research was also made possible through the NIH Medical Research Scholars Program, a public-private partnership supported jointly by the NIH and generous contributions to the Foundation for the NIH from the Doris Duke Charitable Foundation, the American Association for Dental Research, the Colgate-Palmolive Company, Genentech, Elsevier, and other private donors.

Compliance with ethical standard

Funding This project has been funded in whole or in part with federal funds from the National Cancer Institute, National Institutes of Health, under Contract No. HHSN261200800001E. The content of this publication does not necessarily reflect the views or policies of the Department of Health and Human Services, nor does mention of trade names, commercial products, or organizations imply endorsement by the U.S. Government. This research was also made possible through the NIH Medical Research Scholars Program, a public-private partnership supported jointly by the NIH and generous contributions to the Foundation for the NIH from the Doris Duke Charitable Foundation, the American Association for Dental Research, the Colgate-Palmolive Company, Genentech, Elsevier, and other private donors.

Conflict of interest None of the authors (CPS, MC, SM, SH, RS, PLC, BT) of this manuscript have any conflict of interest.

Ethical approval This article does not contain any studies with human participants performed by any of the authors.

Informed consent Not applicable.

References

1. Lambin P, Rios-Velazquez E, Leijenaar R, et al. (2012) Radiomics: extracting more information from medical images using advanced feature analysis. Eur J Cancer. 48(4):441–446
2. Kumar V, Gu Y, Basu S, et al. (2012) Radiomics: the process and the challenges. Magn Reson Imaging. 30(9):1234–1248
3. Thompson I, Thrasher JB, Aus G, et al. (2007) Guideline for the management of clinically localized prostate cancer: 2007 update. J Urol. 177(6):2106–2131
4. Fernandes ET, Sundaram CP, Long R, Soltani M, Ercole CJ (1997) Biopsy Gleason score: how does it correlate with the final pathological diagnosis in prostate cancer? Br J Urol. 79(4):615–617
5. Kvåle R, Møller B, Wahlqvist R, et al. (2009) Concordance between Gleason scores of needle biopsies and radical prostatectomy specimens: a population-based study. BJU Int. 103(12):1647–1654
6. Siddiqui MM, Rais-Bahrami S, Turkbey B, et al. (2015) Comparison of MR/ultrasound fusion-guided biopsy with ultrasound-guided biopsy for the diagnosis of prostate cancer. JAMA. 313(4):390–397
7. Aihara M, Wheeler TM, Ohori M, Scardino PT (1994) Heterogeneity of prostate cancer in radical prostatectomy specimens. Urology. 43(1):60–66 ((discussion 6-7))
8. El-Shater Bosaily A, Valerio M, Hu Y, et al. (2016) The concordance between the volume hotspot and the grade hotspot: a 3-D reconstructive model using the pathology outputs from the PROMIS trial. Prostate Cancer Prostatic Dis. 19(3):258–263
9. Boutros PC, Fraser M, Harding NJ, et al. (2015) Spatial genomic heterogeneity within localized, multifocal prostate cancer. Nat Genet. 47(7):736–745
10. Weinreb JC, Barentsz JO, Choyke PL, et al. (2016) PI-RADS prostate imaging–reporting and data system: 2015, version 2. Eur Urol. 69(1):16–40
11. Greer MD, Brown AM, Shih JH, et al. (2017) Accuracy and agreement of PI-RADS v2 for prostate cancer mpMRI: a multi-reader study. J Magn Reson Imaging. 45(2):579–585
12. Langer DL, van der Kwast TH, Evans AJ, et al. (2010) Prostate tissue composition and MR measurements: investigating the relationships between ADC, T2, K(trans), v(e), and corresponding histologic features. Radiology. 255(2):485–494
13. Zelhof B, Pickles M, Liney G, et al. (2009) Correlation of diffusion-weighted magnetic resonance data with cellularity in prostate cancer. BJU Int. 103(7):883–888
14. Gibbs P, Liney GP, Pickles MD, et al. (2009) Correlation of ADC and T2 measurements with cell density in prostate cancer at 3.0 Tesla. Invest Radiol. 44(9):572–576
15. Haralick RM, Shanmugam K, Dinstein I (1973) Textural features for image classification. IEEE Trans Syst Man Cybernet. 6:610–621
16. Srinivasan G, Shobha G, editors. Statistical texture analysis. Proceedings of world academy of science, engineering and technology; 2008.
17. Bovik AC, Clark M, Geisler WS (1990) Multichannel texture analysis using localized spatial filters. IEEE Trans Pattern Anal Mach Intell. 12(1):55–73
18. Busch C (1997) Wavelet based texture segmentation of multimodal tomographic images. Comput Gr. 21(3):347–358
19. Tang X (1998) Texture information in run-length matrices. IEEE Trans Image Process. 7(11):1602–1609
20. Sun C, Wee W (1983) Neighboring gray level dependence matrix for texture classification. Comput Vis Gr Image Process 23(3):341–352
21. Amadasun M, King R (1989) Texural features corresponding to textural properties. IEEE Trans Syst Man Cybern 23(3):1264–1274
22. Orlhac F, Soussan M, Maisonobe JA, et al. (2014) Tumor texture analysis in 18F-FDG PET: relationships between texture parameters, histogram indices, standardized uptake values, metabolic volumes, and total lesion glycolysis. J Nucl Med. 55(3):414–422
23. Chalkidou A, O'Doherty MJ, Marsden PK (2015) False discovery rates in PET and CT studies with texture features: a systematic review. PLoS One. 10(5):e0124165
24. Trabulsi EJ, Liu XS, Smith WR, Das AK (2013) Transrectal ultrasound of the prostate. In: Gilbert BR, Fulgham PF (eds) *Practical urological ultrasound.* New York: Springer, pp 155–170
25. Shen D, Lao Z, Zeng J, et al. (2004) Optimized prostate biopsy via a statistical atlas of cancer spatial distribution. Med Image Anal. 8(2):139–150
26. Zhan Y, Shen D, Zeng J, et al. (2007) Targeted prostate biopsy using statistical image analysis. IEEE Trans Med Imaging. 26(6):779–788
27. Xu S, Kruecker J, Turkbey B, et al. (2008) Real-time MRI-TRUS fusion for guidance of targeted prostate biopsies. Comput Aided Surg. 13(5):255–264
28. Wu P, Liu Y, Li Y, Liu B (2015) Robust prostate segmentation using intrinsic properties of TRUS images. IEEE Trans Med Imaging. 34(6):1321–1335
29. Gong L, Pathak SD, Haynor DR, Cho PS, Kim Y (2004) Parametric shape modeling using deformable superellipses for prostate segmentation. IEEE Trans Med Imaging. 23(3):340–349
30. K. Diaz, B. Castaneda (eds) *Semi-automated segmentation of the prostate gland boundary in ultrasound images using a machine learning approach. Medical Imaging* (SPIE, 2008).
31. H. Ning, D. B. Downey, A. Fenster, H. M. Ladak (eds) Prostate surface segmentation from 3D ultrasound images. Proceedings IEEE International Symposium on Biomedical Imaging (2002).
32. Cosío FA (2008) Automatic initialization of an active shape model of the prostate. Med Image Anal. 12(4):469–483
33. Ghose S, Oliver A, Mitra J, et al. (2013) A supervised learning framework of statistical shape and probability priors for automatic prostate segmentation in ultrasound images. Med Image Anal. 17(6):587–600
34. A. Zaim, T. Yi, R. Keck (eds) *Feature-Based Classification of Prostate Ultrasound Images using Multiwavelet and Kernel Support Vector Machines.* 2007 International Joint Conference on Neural Networks (12-17 Aug 2007).
35. Yan P, Xu S, Turkbey B, Kruecker J (2010) Discrete deformable model guided by partial active shape model for TRUS image segmentation. IEEE Trans Biomed Eng. 57(5):1158–1166

36. Murphy G, Haider M, Ghai S, Sreeharsha B (2013) The expanding role of MRI in prostate cancer. AJR Am J Roentgenol. 201(6):1229–1238
37. Toth R, Bloch BN, Genega EM, et al. (2011) Accurate prostate volume estimation using multifeature active shape models on T2-weighted MRI. Acad Radiol. 18(6):745–754
38. Chowdhury N, Toth R, Chappelow J, et al. (2012) Concurrent segmentation of the prostate on MRI and CT via linked statistical shape models for radiotherapy planning. Med Phys. 39(4):2214–2228
39. Shiradkar R, Podder TK, Algohary A, et al. (2016) Radiomics based targeted radiotherapy planning (Rad-TRaP): a computational framework for prostate cancer treatment planning with MRI. Radiat Oncol. 11(1):148
40. Pasquier D, Lacornerie T, Vermandel M, et al. (2007) Automatic segmentation of pelvic structures from magnetic resonance images for prostate cancer radiotherapy. Int J Radiat Oncol Biol Phys. 68(2):592–600
41. Costa MJ, Delingette H, Novellas S, Ayache N (2007) Automatic segmentation of bladder and prostate using coupled 3D deformable models. Med Image Comput Comput Assist Interv. 10(Pt 1):252–260
42. Klein S, van der Heide UA, Lips IM, et al. (2008) Automatic segmentation of the prostate in 3D MR images by atlas matching using localized mutual information. Med Phys. 35(4):1407–1417
43. Makni N, Puech P, Lopes R, et al. (2009) Combining a deformable model and a probabilistic framework for an automatic 3D segmentation of prostate on MRI. Int J Comput Assist Radiol Surg. 4(2):181–188
44. Chandra SS, Dowling JA, Shen KK, et al. (2012) Patient specific prostate segmentation in 3-d magnetic resonance images. IEEE Trans Med Imaging. 31(10):1955–1964
45. Litjens G, Toth R, van de Ven W, et al. (2014) Evaluation of prostate segmentation algorithms for MRI: the PROMISE12 challenge. Med Image Anal. 18(2):359–373
46. Makni N, Iancu A, Colot O, et al. (2011) Zonal segmentation of prostate using multispectral magnetic resonance images. Med Phys. 38(11):6093–6105
47. Litjens G, Debats O, van de Ven W, Karssemeijer N, Huisman H (2012) A pattern recognition approach to zonal segmentation of the prostate on MRI. Lect Notes Comput Sc. 7511:413–420
48. Maan B, van der Heijden F, Futterer JJ (2012) A new prostate segmentation approach using multispectral Magnetic Resonance Imaging and a statistical pattern classifier. Proc Spie. 8314:83142Q
49. Chilali O, Puech P, Lakroum S, et al. (2016) Gland and zonal segmentation of prostate on T2W MR images. J Digit Imaging. 29(6):730–736
50. Padgett K, Swallen A, Nelson A, Pollack A, Stoyanova R (2016) Robust atlas based segmentation of the prostate and peripheral zone regions on MRI utilizing multiple MRI system vendors. Med Phys. 43(6):3447
51. Cameron A, Khalvati F, Haider MA, Wong A (2016) MAPS: a quantitative radiomics approach for prostate cancer detection. IEEE Trans Biomed Eng. 63(6):1145–1156
52. Ginsburg SB, Algohary A, Pahwa S, et al. (2017) Radiomic features for prostate cancer detection on MRI differ between the transition and peripheral zones: preliminary findings from a multi-institutional study. J Magn Reson Imaging. 46(1):184–193
53. Han SM, Lee HJ, Choi JY (2008) Computer-aided prostate cancer detection using texture features and clinical features in ultrasound image. J Digit Imaging. 21(Suppl 1):S121–S133
54. Hussain L, Ahmed A, Saeed S, et al. (2018) Prostate cancer detection using machine learning techniques by employing combination of features extracting strategies. Cancer Biomark. 21(2):393–413
55. Khalvati F, Wong A, Haider MA (2015) Automated prostate cancer detection via comprehensive multi-parametric magnetic resonance imaging texture feature models. BMC Med Imaging. 15:27
56. Kwak JT, Xu S, Wood BJ, et al. (2015) Automated prostate cancer detection using T2-weighted and high-b-value diffusion-weighted magnetic resonance imaging. Med Phys. 42(5):2368–2378
57. Lay N, Tsehay Y, Greer MD, et al. (2017) Detection of prostate cancer in multiparametric MRI using random forest with instance weighting. J Med Imaging (Bellingham). 4(2):024506
58. Lopes R, Ayache A, Makni N, et al. (2011) Prostate cancer characterization on MR images using fractal features. Med Phys. 38(1):83–95
59. Madabhushi A, Feldman MD, Metaxas DN, Tomaszeweski J, Chute D (2005) Automated detection of prostatic adenocarcinoma from high-resolution ex vivo MRI. IEEE Trans Med Imaging. 24(12):1611–1625
60. Metzger GJ, Kalavagunta C, Spilseth B, et al. (2016) Detection of prostate cancer: quantitative multiparametric MR imaging models developed using registered correlative histopathology. Radiology. 279(3):805–816
61. Mohamed SS, Li J, Salama MM, Freeman G (2009) Prostate tissue texture feature extraction for suspicious regions identification on TRUS images. J Digit Imaging. 22(5):503–518
62. Stember JN, Deng FM, Taneja SS, Rosenkrantz AB (2014) Pilot study of a novel tool for input-free automated identification of transition zone prostate tumors using T2- and diffusion-weighted signal and textural features. J Magn Reson Imaging. 40(2):301–305
63. Castellano G, Bonilha L, Li LM, Cendes F (2004) Texture analysis of medical images. Clin Radiol. 59(12):1061–1069
64. Lv D, Guo X, Wang X, Zhang J, Fang J (2009) Computerized characterization of prostate cancer by fractal analysis in MR images. J Magn Reson Imaging. 30(1):161–168
65. Wang J, Wu CJ, Bao ML, et al. (2017) Machine learning-based analysis of MR radiomics can help to improve the diagnostic performance of PI-RADS v2 in clinically relevant prostate cancer. Eur Radiol. 27(10):4082–4090
66. Smith AD, Shah SN, Rini BI, Lieber ML, Remer EM (2010) Morphology, Attenuation, Size, and Structure (MASS) criteria: assessing response and predicting clinical outcome in metastatic renal cell carcinoma on antiangiogenic targeted therapy. AJR Am J Roentgenol. 194(6):1470–1478
67. Fehr D, Veeraraghavan H, Wibmer A, et al. (2015) Automatic classification of prostate cancer Gleason scores from multiparametric magnetic resonance images. Proc Natl Acad Sci USA 112(46):E6265–E6273
68. Nketiah G, Elschot M, Kim E, et al. (2017) T2-weighted MRI-derived textural features reflect prostate cancer aggressiveness: preliminary results. Eur Radiol. 27(7):3050–3059
69. Muller BG, Shih JH, Sankineni S, et al. (2015) Prostate Cancer: Interobserver Agreement and Accuracy with the Revised Prostate Imaging Reporting and Data System at Multiparametric MR Imaging. Radiology. 277(3):741–750
70. Mazurowski MA (2015) Radiogenomics: what it is and why it is important. J Am Coll Radiol. 12(8):862–866
71. Incoronato M, Aiello M, Infante T, et al. (2017) Radiogenomic analysis of oncological data: a technical survey. Int J Mol Sci. 18(4):805
72. Rutman AM, Kuo MD (2009) Radiogenomics: creating a link between molecular diagnostics and diagnostic imaging. Eur J Radiol. 70(2):232–241
73. Stoyanova R, Takhar M, Tschudi Y, et al. (2016) Prostate cancer radiomics and the promise of radiogenomics. Transl Cancer Res. 5(4):432–447
74. Thawani R, McLane M, Beig N, et al. (2018) Radiomics and radiogenomics in lung cancer: A review for the clinician. Lung Cancer. 115:34–41
75. Wu J, Tha KK, Xing L, Li R (2018) Radiomics and radiogenomics for precision radiotherapy. J Radiat Res. 59(Suppl 1):i25–i31
76. Pinker K, Shitano F, Sala E, et al. (2017) Background, current role, and potential applications of radiogenomics. J Magn Reson Imaging. 47(3):604–620
77. Lambin P, Leijenaar RTH, Deist TM, et al. (2017) Radiomics: the bridge between medical imaging and personalized medicine. Nat Rev Clin Oncol. 14(12):749–762
78. Valdora F, Houssami N, Rossi F, Calabrese M, Tagliafico AS (2018) Rapid review: radiomics and breast cancer. Breast Cancer Res Treat. 169(2):217–229

79. Zhou M, Scott J, Chaudhury B, et al. (2018) Radiomics in brain tumor: image assessment, quantitative feature descriptors, and machine-learning approaches. AJNR Am J Neuroradiol. 39(2):208–216
80. Litjens GJ, Elliott R, Shih NN, et al. (2016) Computer-extracted features can distinguish noncancerous confounding disease from prostatic adenocarcinoma at multiparametric MR imaging. Radiology. 278(1):135–145
81. Gillies RJ, Kinahan PE, Hricak H (2016) Radiomics: images are more than pictures, they are data. Radiology. 278(2):563–577
82. Vignati A, Mazzetti S, Giannini V, et al. (2015) Texture features on T2-weighted magnetic resonance imaging: new potential biomarkers for prostate cancer aggressiveness. Phys Med Biol. 60(7):2685–2701
83. Wibmer A, Hricak H, Gondo T, et al. (2015) Haralick texture analysis of prostate MRI: utility for differentiating non-cancerous prostate from prostate cancer and differentiating prostate cancers with different Gleason scores. Eur Radiol. 25(10):2840–2850
84. Ahmed HU, El-Shater Bosaily A, Brown LC, et al. (2017) Diagnostic accuracy of multi-parametric MRI and TRUS biopsy in prostate cancer (PROMIS): a paired validating confirmatory study. Lancet. 389(10071):767–768
85. Arsov C, Rabenalt R, Blondin D, et al. (2015) Prospective randomized trial comparing magnetic resonance imaging (MRI)-guided In-bore Biopsy to MRI-ultrasound fusion and transrectal ultrasound-guided prostate biopsy in patients with prior negative biopsies. Eur Urol. 68(4):713–720
86. Bergdahl AG, Wilderang U, Aus G, et al. (2016) Role of magnetic resonance imaging in prostate cancer screening: a pilot study within the goteborg randomised screening trial. Eur Urol. 70(4):566–573
87. Porpiglia F, Manfredi M, Mele F, et al. (2016) Diagnostic pathway with multiparametric magnetic resonance imaging versus standard pathway: results from a randomized prospective study in biopsy-naive patients with suspected prostate cancer. Eur Urol. 72(2):282–288
88. Tonttila PP, Lantto J, Paakko E, et al. (2016) Prebiopsy multiparametric magnetic resonance imaging for prostate cancer diagnosis in biopsy-naive men with suspected prostate cancer based on elevated prostate-specific antigen values: results from a randomized prospective blinded controlled trial. Eur Urol. 69(3):419–425
89. Schena M, Shalon D, Davis RW, Brown PO (1995) Quantitative monitoring of gene expression patterns with a complementary DNA microarray. Science. 270(5235):467–470
90. Marzancola MG, Sedighi A, Li PC (2016) DNA microarray-based diagnostics. Methods Mol Biol. 1368:161–178
91. Geybels MS, Wright JL, Bibikova M, et al. (2016) Epigenetic signature of Gleason score and prostate cancer recurrence after radical prostatectomy. Clin Epigenet. 8:97
92. Poustka A, Pohl T, Barlow DP, et al. (1986) Molecular approaches to mammalian genetics. Cold Spring Harb Symp Quant Biol. 51(Pt 1):131–139
93. Wei L, Wang J, Lampert E, et al. (2016) Intratumoral and intertumoral genomic heterogeneity of multifocal localized prostate cancer impacts molecular classifications and genomic prognosticators. Eur Urol. 71(2):183–192
94. Wyatt AW, Azad AA, Volik SV, et al. (2016) Genomic alterations in cell-free dna and enzalutamide resistance in castration-resistant prostate cancer. JAMA Oncol. 2(12):1598–1606
95. el Bahassi M, Stambrook PJ (2014) Next-generation sequencing technologies: breaking the sound barrier of human genetics. Mutagenesis. 29(5):303–310
96. McCann SM, Jiang Y, Fan X, et al. (2016) Quantitative multiparametric MRI features and PTEN expression of peripheral zone prostate cancer: a pilot study. AJR Am J Roentgenol. 206(3):559–565
97. Stoyanova R, Pollack A, Takhar M, et al. (2016) Association of multiparametric MRI quantitative imaging features with prostate cancer gene expression in MRI-targeted prostate biopsies. Oncotarget. 7(33):53362–53376
98. Aerts HJ (2016) The potential of radiomic-based phenotyping in precision medicine: a review. JAMA Oncol. 2(12):1636–1642
99. The Cancer Genome Atlas (TCGA). Available from: https://cancergenome.nih.gov/. Accessed 12 March 2018
100. The Cancer Imaging Archive (TCIA). Available from: http://www.cancerimagingarchive.net/. Accessed 12 March 2018